Phenotypic Spectrum Caused by Transgenic Overexpression of Activated Akt in the Heart

THE JOURNAL OF BIOLOGICAL CHEMISTRY
Vol. 277, No. 25, Issue of June 21, pp. 22896–22901, 2002

Printed in U.S.A.

Phenotypic Spectrum Caused by Transgenic Overexpression of Activated Akt in the Heart*

Received for publication, January 11, 2002, and in revised form, April 5, 2002
Published, JBC Papers in Press, April 9, 2002, DOI 10.1074/jbc.M200347200

Takashi Matsui‡, Ling Li‡, Justina C. Wu§, Stuart A. Cook‡, Tomohisa Nagoshi‡, Michael H. Picard§, Ronglih Liao¶, and Anthony Rosenzweig‡‖

From the ‡Program in Cardiovascular Gene Therapy, CVRC, the §Cardiology Division, Massachusetts General Hospital, Harvard Medical School, Boston, Massachusetts 02129, and the ¶Cardiac Muscle Research Laboratory, Boston University School of Medicine, Boston, Massachusetts 02118

The serine-threonine kinase, Akt, inhibits cardiomyocyte apoptosis acutely both *in vitro* and *in vivo*. However, the effects of chronic Akt activation in the heart are unknown. To address this issue, we generated transgenic mice (TG+) with cardiac-specific expression of a constitutively active mutant of Akt (myr-Akt) driven by the myosin heavy chain-α promoter. Three TG+ founders (9–19 weeks) died suddenly with massive cardiac dilatation. Two viable TG+ lines (TG564 and TG20) derived from independent founders demonstrated cardiac-specific transgene expression as well as activation of Akt and p70S6 kinase. TG564 ($n = 19$) showed cardiac hypertrophy with a heart/body weight ratio 2.3-fold greater than littermates ($n = 17, p < 0.005$). TG20 ($n = 18$) had less marked cardiac hypertrophy with a heart/body weight ratio 1.6-fold greater than littermates ($n = 17, p < 0.005$). Isolated TG564 myocytes were also hypertrophic with surface areas 1.7-fold greater than littermates ($p < 0.000001$). Echocardiograms in both lines demonstrated concentric hypertrophy and preserved systolic function. After ischemia-reperfusion, TG+ had a 50% reduction in infarct size *versus* TG− (17 ± 3% *versus* 34 ± 4%, $p < 0.001$). Thus, chronic Akt activation is sufficient to cause a spectrum of phenotypes from moderate cardiac hypertrophy with preserved systolic function and cardioprotection to massive cardiac dilatation and sudden death.

The serine-threonine kinase, Akt (or protein kinase B), appears critically positioned between a variety of stimuli and effectors relevant to cardiac function in normal and diseased hearts. Akt is activated by many cardioprotective ligand-receptor systems including insulin (1, 2), insulin-like growth factor-I (3–6), gp130-dependent cytokines (7, 8), and estrogen (9). Acute Akt activation itself protects cardiomyocytes from apoptosis *in vitro* (10) and *in vivo* (11, 12), while dramatically reducing infarction and cardiac dysfunction 24 h after transient ischemia (12). However, the chronic effects of Akt activation in the heart are unknown.

In most systems, Akt activation occurs downstream of the lipid kinase, PI 3-kinase,[1] itself a powerful anti-apoptotic signal (1–8, 10). Signaling downstream of PI 3-kinase is complex and includes mitogen-activated protein kinases and p70S6 kinase, in addition to Akt, and appears to modulate many important cell processes including cell metabolism and growth (13, 14). In *Drosophila*, PI 3-kinase is a critical determinant of organ size and development (15), and recent work suggests it plays a similar role in the mammalian heart (16). The downstream pathways responsible for controlling cardiomyocyte size have not been identified.

Activation of PI 3-kinase leads to D3 phosphorylation of membrane phosphatidylinositol 4,5-bisphosphate, generating phosphatidylinositol 3,4,5-trisphosphate, some of which is converted to phosphatidylinositol 3,4-trisphosphate by an inositol phosphatase (17). Phosphatidylinositol 3,4-trisphosphate and phosphatidylinositol 3,4,5-trisphosphate accumulate in the cell membrane and recruit Akt and PDK1 to the cell membrane by binding to their pleckstrin homology domains, leading to phosphorylation and activation of Akt (18). Because PDK1 is constitutively active, movement of Akt to the sarcolemmal membrane is sufficient to lead to its activation. For this reason, incorporation of the *src* myristoylation signal creates a constitutively active Akt mutant (10). Downstream substrates of Akt mediate important effects on a broad range of cell functions including cell survival (19–21), inflammation (22–25), and metabolism (26, 27). The relative contribution of these downstream effectors in mediating the cardiac effects of Akt remains undefined.

To examine the effects of chronic Akt activation in the heart, we generated transgenic mice with cardiac overexpression of a constitutively active mutant of Akt (myr-Akt). Mice demonstrated a broad spectrum of phenotypes from sudden death with massive cardiac enlargement to cardiac hypertrophy with preserved systolic function and protection from ischemia-reperfusion injury. Two viable lines have been bred for five generations and characterized more fully. These lines should provide a valuable tool for investigating the effects of Akt activation in chronic models of cardiac disease.

EXPERIMENTAL PROCEDURES

Generation of Transgenic Mice

The cDNA encoding HA-tagged Akt with Src myristoylation (myr) signal (kindly provided by Dr. Thomas F. Franke, Columbia University) was subcloned downstream of the 5.5-kb murine α-myosin heavy chain

* This work was supported in part by National Institutes of Health Grants HL04250 (to T. M.) and HL59521 and HL61557 (to A. R.). The costs of publication of this article were defrayed in part by the payment of page charges. This article must therefore be hereby marked "*advertisement*" in accordance with 18 U.S.C. Section 1734 solely to indicate this fact.

‖ Established Investigator of the American Heart Association. To whom correspondence should be addressed: Program in Cardiovascular Gene Therapy, Cardiovascular Research Center, Massachusetts General Hospital, EAST, 114 16th St., 2nd Floor, Rm. 2600, Charlestown, MA 02129. Tel.: 617-726-8286; Fax: 617-726-5806; E-mail: rosenzweig@helix.mgh.harvard.edu.

[1] The abbreviations used are: PI 3-kinase, phosphatidylinositol 3-kinase; HA, hemagglutinin; ERK, extracellular signal-regulated kinase; SAPK, stress-activated protein kinase; JNK, c-Jun NH_2-terminal kinase; MOPS, 4-morpholinepropanesulfonic acid; Ab, antibody; GSK-3, glycogen synthase kinase-3.

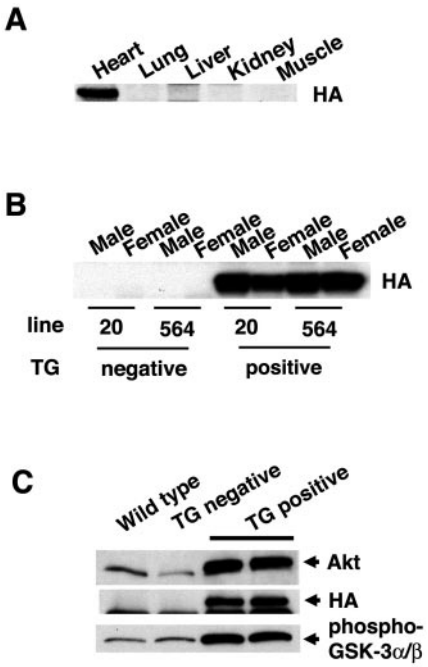

FIG. 1. **Overexpression of myr-Akt in the heart.** *A,* cardiac overexpression of HA-tagged myr-Akt. Twenty μg of whole lysates from various organs in TG20 were separated by SDS-PAGE. Transgene expression was analyzed by Western blotting, using a monoclonal antibody to the HA epitope. The transgene was expressed in the heart but not in the lung, kidney, or skeletal muscle. Representative data from one of three independent experiments are shown. In TG564, slight expression of transgene was detected in the lung as well (data not shown). *B,* expression pattern in female and male transgenic mice. Immunoblotting was performed as above. Transgene expression in TG20 females was significantly less than in TG20 males. No difference was seen in transgene expression between female and male TG564 mice. *C,* Akt kinase activity. Akt kinase activity was examined with homogenates from wild type, TG−, and TG564+ hearts, using the GSK-3α/β fusion protein as substrate, as described under "Experimental Procedures." The overall level of Akt expression was significantly increased in TG564+ mice (*top*), as was Akt kinase activity (bottom). Representative immunoblots of two separate experiments, total four independent TG+ mice, are shown.

promoter (generously given by Dr. Jeffrey Robbins, Division of Molecular Cardiovascular Biology, Cincinnati Children's Hospital Research Foundation (28)) and used to generate transgenic mice through oocyte injection. Positive founders were identified by Southern blotting and bred to wild-type C57BL6 mice.

Western Blotting

Hearts from 8–16-week old mice were removed from deeply anesthetized animals, snap frozen, and crushed in liquid nitrogen before tissue was homogenized in cold lysis buffer (20 mM Tris-HCl (pH 7.6), 150 mM NaCl, 1% Triton X-100, 2 mM EGTA, 1 mM phenylmethylsulfonyl fluoride, 1 mM dithiothreitol, 1 mM sodium orthovanadate, 1 μg/ml leupeptin, 1 μg/ml aprotinin). Protein concentration was measured by the Bradford method (Bio-Rad). SDS-PAGE was performed under reducing conditions on 12% separation gels with a 4% stacking gel. Proteins were transferred to nitrocellulose membrane. Blots were incubated with primary antibodies to HA (12CA5, Roche Molecular Biochemicals), Akt (Cell Signaling), phospho-Akt (Ser-473, Cell Signaling), ERK1/2 (Santa Cruz), phospho-ERK1/2 (Cell Signaling), GSK-3β (Transduction Lab), phospho-GSK-3β (Cell Signaling), SAPK/JNK (Cell Signaling), p38 (Cell Signaling), phospho-p70S6 kinase (Cell Signaling), and p70S6 kinase (Cell Signaling) for 18–20 h at 4 °C. Blots were then incubated with horseradish peroxidase-conjugated secondary antibody and signal detected using enhanced chemiluminescence (Cell Signaling).

Kinase Assays

Akt Kinase Assay—Myocardial tissue was lysed, immunoprecipitated with anti-Akt antibody, and used to measure Akt kinase activity using the Akt Kinase Assay Kit (Cell Signaling) with GSK-3α/β as substrate, according to the manufacturer's instructions.

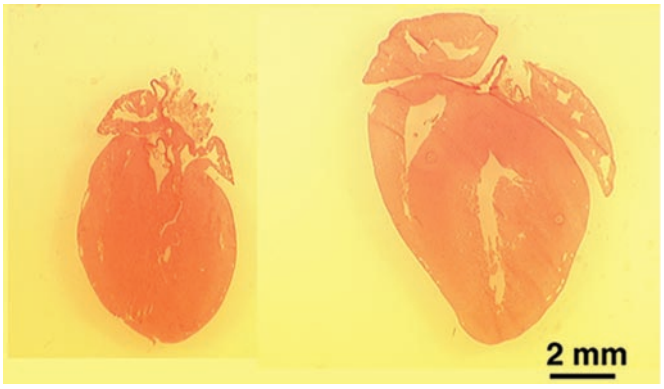

FIG. 2. **Constitutively active Akt induces cardiac hypertrophy.** Sections obtained from hearts of 12-week-old TG− and TG+ littermates from the TG564 line, stained with hematoxylin and eosin, are shown. TG+ heart (*right*) demonstrates dramatic concentric hypertrophy.

JNK and p38 Kinase Assay—These kinase activities were measured with the SAPK/JNK and p38 kinase Assay Kits (Cell Signaling) using c-Jun and ATF-2 as substrates for SAPK/JNK and p38, respectively, according to the manufacturer's instructions.

GSK-3β–Kinase activity of GSK-3β was measured as described previously (29). Briefly, frozen hearts were homogenized and lysed in the lysis buffer. GSK-3β was immunoprecipitated with anti-GSK-3β monoclonal antibody coupled to protein G-Sepharose beads. After the beads were washed, the immunoprecipitates were incubated for 20 min at 30 °C in reaction mixture containing 25 mM β-glycerophosphate, 20 mM MOPS (pH 7.2), 10 mM $MgCl_2$, 2 mM EGTA, 0.5 μM protein kinase inhibitor, 1 mM dithiothreitol, 50 μM unlabeled ATP, 5 μCi of [γ-^{32}P]ATP, and 50 μM glycogen synthase peptide-2 (Upstate) as substrate. The mixtures were spotted onto Whatman P81 paper, washed with 0.5% phosphoric acid, and ^{32}P measured by liquid scintillation spectroscopy. Kinase activity was reduced to background levels when 10 mM LiCl was included in the reaction mixture, suggesting the activity measured was GSK-3β (data not shown).

p70S6 Kinase Assay—Lysates were prepared as above and immunoprecipitated with Ab to p70S6 kinase (Cell Signaling). The immobilized immunoprecipitates were washed with HEPES-buffered saline (pH 7.5) containing 0.1% Triton X-100 and incubated for 30 min at 25 °C in reaction mixture containing 25 mM MOPS (pH 7.2), 12 mM $MgCl_2$, 2 mM EGTA, 0.5 mM dithiothreitol, 10 mM β-glycerol phosphate, 0.5 μM protein kinase inhibitor, 100 μM unlabeled ATP, 2 μCi of [γ-^{32}P]ATP, 100 μM S6 synthetic peptide (RRLSSLRA; Alexis Biochemical) as substrate. The reaction mixtures were spotted on P81 paper and washed with 0.5% phosphoric acid. ^{32}P incorporation into the peptide was determined by liquid scintillation spectroscopy. For all kinase assays, samples from 8–16-week old mice were used.

Histochemical Examination

Tissues were snap-frozen in OCT medium, and 10-μm sections were prepared for hematoxylin and eosin staining. Morphological analysis of hematoxylin and eosin-stained tissue was performed using microscopy and a SONY imaging system.

Cardiomyocyte Isolation

Left ventricular cardiomyocytes were isolated with the perfused-heart method described previously (30). Briefly, after deeply anesthetizing the mice, hearts were quickly excised, cannulated via the aorta, and perfused in the Langendorff mode with a constant perfusion pressure of 80 mm Hg. The hearts were first perfused for 5 min at 37 °C with 1.8 mM Ca^{2+} Tyrode (in mM: NaCl 137, KCl 5.4, $CaCl_2$ 1.8, $MgCl_2$ 0.5, HEPES 10, and glucose 10, pH 7.4), followed by Ca^{2+}-free Tyrode for an additional 5 min. They were then perfused with a digestion solution containing 5 mg of collagenase D (Roche Molecular Biochemicals), 17.5 mg of collagenase B (Roche Molecular Biochemicals), and 1.5 mg of protease XIV (Sigma) in 35 ml of Ca^{2+}-free Tyrode. After the hearts were palpably flaccid, the digestion solution was washed out with Ca^{2+}-free Tyrode solution for 30 s. The left ventricle (including the septum) was cut into small pieces and gently agitated, allowing the myocytes to be dispersed in Ca^{2+}-free Tyrode. The isolated myocytes were then fixed with 2% paraformaldehyde for 15 min and washed with phosphate-buffered saline. Using Cytospin2 (Shandon Inc., Pittsburgh),

TABLE I
Heart and body weight of TG mice

n = number of animals. Data are mean ± S.E.

	Negative littermates (20 line)		Negative littermates (564 line)	
	Female (n = 8)	Male (n = 9)	Female (n = 9)	Male (n = 8)
Age (weeks)	15.0 ± 1.2	14.5 ± 2.4	14.1 ± 0.7	14.5 ± 0.5
Body weight (g)	24.7 ± 0.9	30.4 ± 2.4	23.4 ± 0.9	30.4 ± 1.7
Heart weight (mg)	111.7 ± 3.5	128.0 ± 3.4	102.5 ± 4.8	130.1 ± 0.5
HW/BW (mg/g)	4.5 ± 0.1	4.3 ± 0.2	4.4 ± 0.2	4.3 ± 0.2
	TG20 positive		TG564 positive	
	Female (n = 8)	Male (n = 10)	Female (n = 10)	Male (n = 9)
Age (weeks)	16.7 ± 2.3	16.6 ± 1.0	15.8 ± 1.7	15.4 ± 1.3
Body weight (g)	25.1 ± 1.5	29.5 ± 1.9	24.5 ± 1.3	29.6 ± 1.7
Heart weight (mg)	175.3 ± 11.5[a]	209.3 ± 11.8[a]	268.1 ± 15.9[a,b]	262.9 ± 8.3[a,b]
HW/BW (mg/g)	7.0 ± 0.4[a]	7.2 ± 0.3[a]	11.0 ± 0.4[a,b]	9.0 ± 0.5[a,b]

[a] $p < 0.005$ *versus* negative animals.
[b] $p < 0.005$ *versus* the same gender in 20 line.

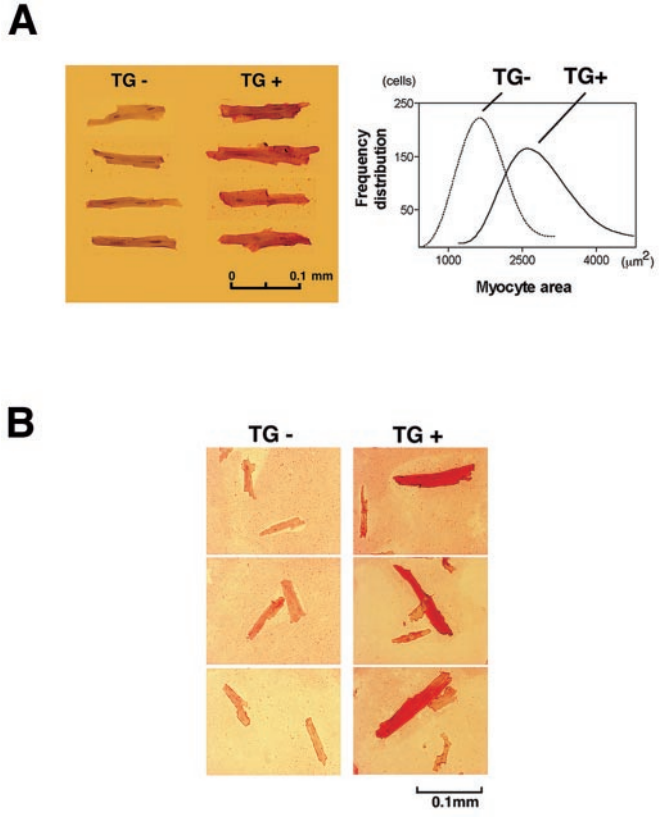

FIG. 3. **Akt activation induces cardiomyocyte hypertrophy.** *A,* cardiomyocyte area in TG564 mice. Isolated cardiomyocytes were stained for the HA epitope. All cells from TG564 positive hearts expressed the transgene, while no staining was seen in transgene negative littermates. Surface area of 300 cells from two individual mice was measured using NIH image and plotted on the graph (*right*). *B,* cardiomyocytes from TG20 mice. Isolated cardiomyocytes from TG20 female mice demonstrated size heterogeneity. Large cells stained positive for transgene expression while the smaller cardiomyocytes did not.

myocytes suspended with phosphate-buffered saline were placed on glass slides and stained with anti-HA Ab. The Ab was detected using Vectastain ABC-Alkaline Phosphatase kit (VECTOR Lab). Images were digitally captured, and individual cells were traced and surface areas calculated using NIH image (version 1.60).

Echocardiography

Mice were anesthetized with ketamine (100 mg/kg intraperitoneal injection) and the anterior chest was shaved. Cardiac ultrasound imaging was performed in the left lateral decubitus position using a high-frequency 13.0 MHz liner transducer (Acuson Sequoia C256 with a 15L8 linear array) at a frame rate of 166 frames/s and imaging depth set at 10 mm. Estimated ejection fraction was calculated using a modified Simpson's rule.

Ischemia-Reperfusion Model

TG20 male positive and negative littermates aged 9–12 weeks were subjected to ischemia-reperfusion as previously described (12). Briefly, seven animals from each group were anesthetized (Avertin), intubated, and ventilated. Left thoracotomy was performed and LAD ligated with 7-0 silk. 5 min into ischemia, 50 μl of fluorescent microspheres (10-μm FluoSpheres, Molecular Probes) were injected into the LV cavity. After 30 min, the LAD ligature was released, and reperfusion visually confirmed. Mice were sacrificed 24 h after ischemia. Hearts were frozen in liquid N_2, and sectioned from apex to base (Jung Frigocut 2800E, Leica) into four 2-mm sections. To delineate the infarct, sections were incubated in 5% (w/v) triphenyltetrazolium chloride (Sigma) in phosphate-buffered saline (pH 7.4) at 37 °C for 20 min. The area-at-risk delineated by fluorescent microspheres was visualized under UV light. For each section, the area-at-risk and infarct area were measured from enlarged digital micrographs using NIH image. %MI was calculated as the total infarction area divided by the total area-at-risk for that heart.

Statistical Analysis

Data are presented as the mean ± S.E. from at least three independent experiments and were compared using a two-tailed Student's t test. The null hypothesis was rejected at $p < 0.05$.

RESULTS

Generation of myr-Akt Mice—Cardiac specific expression of constitutively active Akt (myr-Akt) was driven by the murine α-myocin heavy chain promoter, which produces predominantly postnatal ventricular transgene expression (28). Three transgene positive (TG+) founders (two females, one male) died suddenly with massive cardiac dilatation at ages 9–19 weeks. Two viable TG+ lines (TG564 and TG20) were derived from independent founders. Both lines exhibited Mendelian inheritance of the transgene consistent with autosomal (TG564) and X-linked (TG20) transmission stable over 5 generations (data not shown). Western blotting using a monoclonal antibody to the incorporated HA epitope confirmed cardiac-specific expression (Fig. 1*A*). Transgene expression was comparable in TG564 male and female mice. In TG20 mice, transgene expression was greater in male compared with female mice (Fig. 1*B*). Immunohistochemical staining in female TG20 mice revealed that not all cardiomyocytes expressed the transgene (data not shown) consistent with the expected inactivation of the transgene-encoding X-chromosome in some cardiomyocytes. Immunoblotting with monoclonal antibody to Akt demonstrated substantial overexpression of the transgene in comparison to the endogenous molecule (Fig. 1*C*). Akt activity was dramatically increased as measured by an *in vitro* kinase assay using a synthetic GSK-3α/β fusion protein as substrate (Fig. 1*C, bottom*).

TABLE II
Echocardiographic finding in TG mice

n = number of animals. Data are mean ± S.E.

	IVS	PW	EF
	mm		%
Female negative (n = 10)	0.66 ± 0.03	0.64 ± 0.02	68.0 ± 2.4[a]
Male negative (n = 15)	0.73 ± 0.04	0.72 ± 0.04	65.9 ± 1.7[a]
TG20 female positive (n = 13)	0.82 ± 0.03[b]	0.84 ± 0.03[b]	63.8 ± 1.2[a]
TG20 male positive (n = 10)	0.96 ± 0.04[c]	0.98 ± 0.04[c]	62.5 ± 2.8[a]
TG564 female positive (n = 9)	0.97 ± 0.04[c]	1.03 ± 0.03[c]	62.9 ± 1.9[a]
TG564 male positive (n = 8)	0.94 ± 0.05[c]	0.92 ± 0.06[c]	62.0 ± 2.4[a]

The abbreviations are: IVS, intraventricular septum; PW, posterior wall; EF, ejection fraction.
[a] p = not significant.
[b] $p < 0.05$ *versus* female negative animals.
[c] $p < 0.05$ *versus* TG20 female positive.

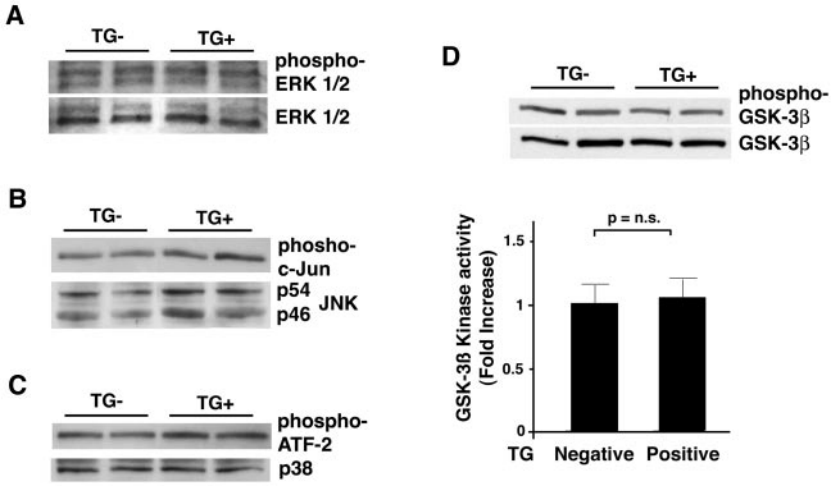

FIG. 4. **Hypertrophic signaling pathways in Akt mice.** *A,* ERK activation. No change in phosphorylated or total ERK1/2 was seen in transgenic Akt mice. *B,* JNK activation. The activation of JNK was evaluated with using c-Jun as substrate. The activity and level of expression of JNK were not changed. *C,* p38 activation. The activation of p38 was evaluated with phosphorylation of ATF-2, as described under "Experimental Procedures." The activity and level of expression of p38 were not changed**.** *D,* GSK-3β activation. Similarly, no change in phosphorylated (Ser^9) or total GSK-3β was seen in transgenic Akt mice (*upper panel*). The GSK-3β kinase activity in TG+ was not significantly different from that seen in littermate controls. Cumulative data from 12 animals (6 in each group) are shown (*lower panel*). All blots shown are from TG564 and represent at least three independent experiments.

Phenotypic Effects of Cardiac Akt Activation—Hearts from transgenic mice in both lines were substantially larger than transgene negative (TG−) littermates with evident gross cardiac hypertrophy (Fig. 2 and Table I). In TG564 mice, the HW/BW ratio was 2.5- and 2.1-fold greater than that seen in TG− female and male littermates ($p < 0.005$), respectively (Table I). TG20 had less marked cardiac hypertrophy with a HW/BW ratio 1.6- and 1.7-fold greater than that seen in TG− female and male littermates ($p < 0.005$), respectively.

To characterize the cardiac enlargement on a cellular level, we isolated cardiomyocytes from transgenic mice and their littermates. Cardiomyocyte surface area was measured from digitized micrographs of isolated cells. TG564 myocytes were substantially larger with a mean surface area 1.7-fold greater than that seen in TG− littermates (2827 ± 30 *versus* 1692 ± 20 μm^2, $p < 0.000001$) (Fig. 3*A*). Cardiomyocytes isolated from TG20 females revealed significant heterogeneity in size. Immunohistochemical staining revealed that the larger cardiomyocytes expressed the Akt transgene, while the smaller cardiomyocytes did not (Fig. 3*B*).

Functional Analysis—Echocardiograms were performed in both lines from 8 to 18 weeks to assess *in vivo* cardiac function as well as wall and chamber dimensions. TG20 mice demonstrated LV hypertrophy that was slightly more marked for male as compared with female TG+ mice (Table II). Wall thickness in TG564 mice was comparably increased in both males and females, and similar to that seen in male TG20 mice. Systolic ventricular function (as indicated by ejection fraction) was normal in both lines (Table II).

Signal Transduction in the myr-Akt Transgenic Mice—Several signaling pathways relevant to cardiac hypertrophy were examined. We observed no change in the level of total extracellular regulated kinases (ERK)-1 and 2, or phosphorylated ERK-1 and –2 (Fig. 4*A*). Stress-activated protein kinase (SAPK/JNK) has also been implicated in cardiac hypertrophy both *in vitro* (31) and *in vivo* (32). Nevertheless, there was no difference between SAPK activity in TG+ and TG− mice (Fig. 4*B*). We measured phosphorylation of p38 and p38 kinase activity with ATF-2 as substrate. Although occasional TG+ mice showed modestly enhanced phosphorylation of p38, most did not (data not shown). Moreover, p38 activity was similar between TG+ and TG− mice (Fig. 4*C*). GSK-3β is phosphorylated and inactivated by Akt (33). GSK-3β inactivation is required for cardiomyocyte hypertrophy in response to some stimuli *in vitro* (29). However, we found no difference in total or phosphorylated GSK-3β between TG+ and TG− mice (Fig. 4*D*, *upper panel*). Similarly, there was no difference in activity (Fig. 4*D*, *lower panel*). The ribosomal protein p70S6 kinase is another downstream target of Akt (34), which regulates translation initiation and has previously been reported to promote cellular growth (35, 36) and hypertrophy (37). Phosphorylation of Thr^{389} correlates well with p70S6 kinase activity (38, 39). In Akt transgenic mice, overall expression of p70S6 kinase was increased, as was phosphorylation at Thr^{389} as well as Thr^{421}/

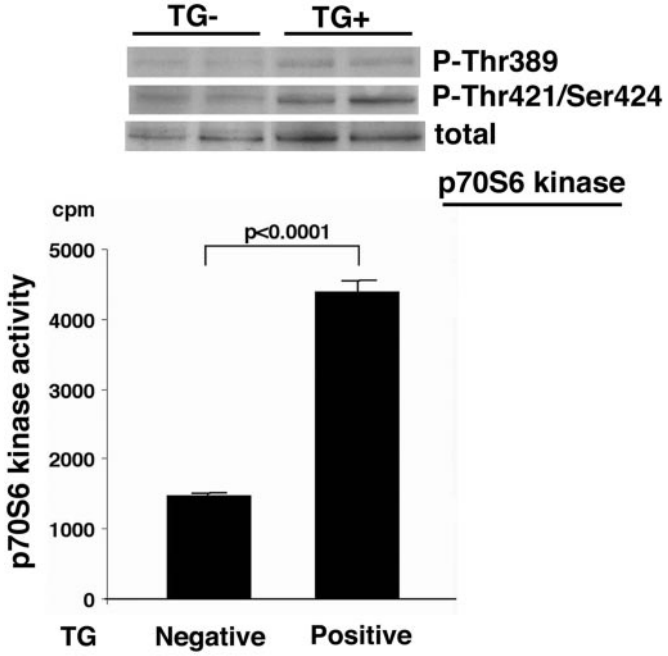

FIG. 5. **p70S6 kinase activation.** Phosphorylation of p70S6 kinase in TG mice (*upper panel*). An increase in both the total (*bottom*) and phosphorylated (Thr^{389} (*top*) and Thr^{421}/Ser^{424} (*middle*)) p70S6 kinase was seen in myr-Akt mice. p70S6 kinase activity in TG mice (*lower panel*). Kinase activity was measured with phosphorylation of the synthetic S6 peptide, as described under "Experimental Procedures." The activation of p70S6 kinase was significantly increased in TG mice. Representative data from one of three independent experiments performed in triplicate are shown.

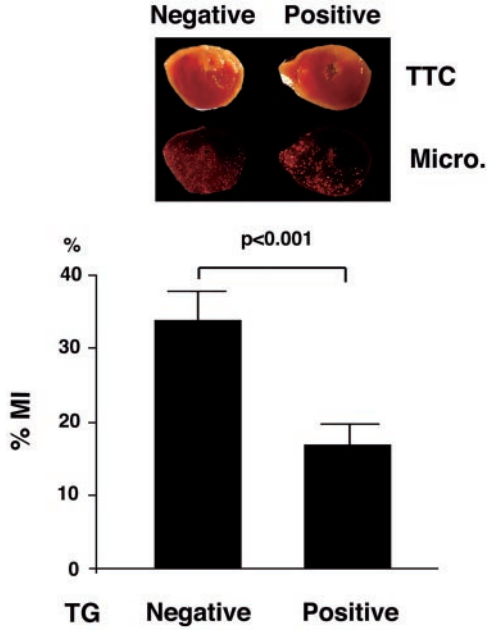

FIG. 6. **myr-Akt mice are protected from ischemia-reperfusion injury.** *Micrograph,* representative fluorescent microsphere distribution (*bottom*) and triphenyltetrazolium chloride staining (*top*) for 1 section from TG− (*left*) or TG+ (*right*). *Graph*, %MI in TG+ was reduced by ≈50% compared with TG− littermates (17 ± 3% *versus* 34 ± 4%, $p < 0.001$). There was no change in area-at-risk (data not shown). Cumulative data from 14 animals (7 in each group) are shown.

Ser^{424} (Fig. 5, *upper panel*). p70S6 kinase activity was also significantly increased in TG+ mice, as measured in a kinase assay using a synthetic S6 peptide as substrate (Fig. 5, *lower panel*).

Ischemia-Reperfusion Injury Model Using TG Mice—We have demonstrated that acute Akt activation prevents ischemia-reperfusion injury after gene transfer (12). To examine whether chronic Akt activation is also cardioprotective, we measured myocardial infarction 24 h after 30 min coronary ligation in TG20 mice (Fig. 6). The ischemic area induced by LAD ligation (%AAR) did not differ between TG+ and TG− (44 ± 3% *versus* 49 ± 4, p = n.s.). However, infarct size was reduced by ≈50% in TG positive mice compared with littermate controls (17 ± 3% *versus* 34 ± 4%) (Fig. 6).

DISCUSSION

In the present study, we have generated transgenic mouse lines with overexpression of constitutively active Akt (myr-Akt) driven by the α-myocin heavy chain promoter (28). Three founders died with massive cardiac dilatation at 9–19 weeks. In contrast, two viable lines demonstrated gross and cellular hypertrophy with preserved systolic function. These lines manifested stable Mendelian inheritance with patterns consistent with autosomal (TG564) and X-linked (TG20) transmission. Myr-Akt was specifically expressed in the hearts of both lines resulting in a dramatic increase in the activity of Akt and its downstream substrate, p70S6 kinase.

Interest in Akt signal transduction has been heightened by the demonstration that Akt activation reduces injury in models of cardiac ischemia (10–12). However, all of these studies were performed using acute viral gene transfer to achieve transient Akt activation and documented benefits on relatively short-term endpoints. An understanding of the effects of chronic Akt activation both at baseline and in disease models may help determine the value of Akt signaling as a therapeutic target. In the current study, three transgenic founders (2F and 1M) with cardiac transgene expression (data not shown) died suddenly with massive cardiac enlargement at ages 9–19 weeks. While detailed quantitative analysis of these animals was not possible, this observation raises the possibility that chronic Akt activation can, under some circumstances, be detrimental. This toxicity may be related to the level of expression achievable with the α-myocin heavy chain promoter. In this context, however, it is worth noting that transgenic cardiac GFP expression has also been reported to induce dilated cardiomyopathy (40), and thus, this phenotype must be interpreted cautiously. On the other hand, two viable lines were produced which demonstrated marked Akt overexpression and dramatic increases in Akt activity that were well tolerated. Thus, while the level of Akt expression and activation are likely to be important considerations, there appears to be a broad range of Akt expression and activation that is well tolerated by the adult mammalian heart.

The construct used for these studies (myr-Akt) is rendered constitutively active by initial localization to the sarcolemma. We have previously shown that gene transfer at the same construct recapitulates many of the signaling and biological effects seen with insulin-like growth factor-I treatment (10). Moreover, after Ad.myr-Akt gene transfer to the heart *in vivo*, the HA-tagged construct is found not only at the sarcolemma but also in the cytosolic fraction (data not shown). Thus, to a large extent, myr-Akt produces a pattern of Akt activation resembling that seen with ligand activation of the endogenous molecule. However, the possibility that subtle differences in subcellular localization affect downstream signaling is worthy of further investigation.

Although PI 3-kinase activity is an important determinant of mammalian heart size (16), the downstream substrates mediating this effect have not been identified. Our data establish that Akt activation is sufficient to cause both cellular and gross hypertrophy and suggest that Akt may well mediate the effects of PI 3-kinase on cardiomyocyte size. The fortuitous finding of

X-linked transmission in TG20 mice allows us to infer that cardiac Akt activation modulates cell size in a primary and cell autonomous manner, rather than secondary to hemodynamic changes or paracrine signals. The observed increase in cardiomyocyte surface area appears to quantitatively account for the entire increase in heart mass (assuming the increase in mass is proportional to volume and thus surface area$^{3/2}$). However, it is difficult to exclude the possibility that cardiomyocyte hyperplasia contributes to the observed increase in cardiac mass. Akt inhibits p21^{CIP1} (41, 42) and thus could affect cardiomyocyte proliferation (43). However, we found no evidence in bromodeoxyuridine incorporation studies for enhanced myocyte proliferation, although bromodeoxyuridine incorporation was evident in the small intestine from treated animals (data not shown). A dominant effect of Akt on cell size rather than number is consistent with prior work in *Drosophila* (44) and a recent study of Akt expression in pancreatic islets (45).

The pathways downstream of Akt that mediate increased cardiomyocyte size have not been fully defined in the current study. We found no change in ERK1/2, SAPK/JNK, p38, or GSK-3β, despite a connection of these signaling pathways to cardiac hypertrophy in other systems (29, 31, 32, 46). Recently it has been reported that inactivation of GSK-3β by Akt induces cardiomyocyte hypertrophy *in vitro* and atrial natriuretic factor expression (29, 47). Interestingly, we did not observe enhanced atrial natriuretic factor in the myr-Akt mice (data not shown). In contrast, both total and phosphorylated p70S6 kinase were increased, as was kinase activity. p70S6 kinase plays an important role in cell size determination in both mammals (35, 36) and *Drosophila* (48). It seems likely that the dramatic increase in p70S6 kinase activity contributes to the observed increase in cell size. Moreover, it is also possible that this pathway contributes to Akt's cytoprotective effects (49).

We have previously demonstrated that *acute* Akt activation reduces infarct size after ischemia-reperfusion. However, it was possible that *chronic* Akt activation would adversely affect the heart's response to transient ischemia. This possibility was underscored by the observed death of 3 founders. Interestingly, in TG20 mice, chronic Akt activation substantially reduced infarction. Further studies will be required to identify the downstream mediators of cardioprotection in this model and determine whether they are the same effectors that protect the heart after acute Akt activation (12).

In addition to providing a tool to dissect Akt mediated signaling events in the heart, the mice described in this study should help us gauge the potential of Akt activation as a therapeutic target. It will be of interest to evaluate the long-term effects of Akt activation. To date, survival and health of both lines appear normal (data not shown). Studies in TG20 and TG564 mice should help address these issues.

Acknowledgments—We thank Dr. Thomas Franke for the myr-Akt cDNA and Dr. Jeffrey Robbins for the α-myocin heavy chain promoter. We also thank Drs. Kazuyoshi Yonezawa, Kenta Hara, and Thomas Force for their helpful advice.

REFERENCES

1. Cong, L. N., Chen, H., Li, Y., Zhou, L., McGibbon, M. A., Taylor, S. I., and Quon, M. J. (1997) *Mol. Endocrinol.* **11,** 1881–1890
2. Baines, C. P., Wang, L., Cohen, M. V., and Downey, J. M. (1999) *Basic Res. Cardiol.* **94,** 188–198
3. Kulik, G., Klippel, A., and Weber, M. J. (1997) *Mol. Cell. Biol.* **17,** 1595–1606
4. Dudek, H., Datta, S. R., Franke, T. F., Birnbaum, M. J., Yao, R., Cooper, G. M., Segal, R. A., Kaplan, D. R., and Greenberg, M. E. (1997) *Science* **275,** 661–665
5. Buerke, M., Murohara, T., Skurk, C., Nuss, C., Tomaselli, K., and Lefer, A. M. (1995) *Proc. Natl. Acad. Sci. U. S. A.* **92,** 8031–8035
6. Li, B., Setoguchi, M., Wang, X., Andreoli, A. M., Leri, A., Malhotra, A., Kajstura, J., and Anversa, P. (1999) *Circ. Res.* **84,** 1007–1019
7. Oh, H., Fujio, Y., Kunisada, K., Hirota, H., Matsui, H., Kishimoto, T., and Yamauchi-Takihara, K. (1998) *J. Biol. Chem.* **273,** 9703–9710
8. Hirota, H., Chen, J., Betz, U. A., Rajewsky, K., Gu, Y., Ross, J., Jr., Muller, W., and Chien, K. R. (1999) *Cell* **97,** 189–198
9. Camper-Kirby, D., Welch, S., Walker, A., Shiraishi, I., Setchell, K. D., Schaefer, E., Kajstura, J., Anversa, P., and Sussman, M. A. (2001) *Circ. Res.* **88,** 1020–1027
10. Matsui, T., Li, L., del Monte, F., Fukui, Y., Franke, T., Hajjar, R., and Rosenzweig, A. (1999) *Circulation* **100,** 2373–2379
11. Fujio, Y., Nguyen, T., Wencker, D., Kitsis, R. N., and Walsh, K. (2000) *Circulation* **101,** 660–667
12. Matsui, T., Tao, J., del Monte, F., Lee, K.-H., Li, L., Picard, M., Force, T. L., Franke, T. F., Hajjar, R. J., and Rosenzweig, A. (2001) *Circulation* **104,** 330–335
13. Coffer, P. J., Jin, J., and Woodgett, J. R. (1998) *Biochem. J.* **335,** 1–13
14. Rameh, L. E., and Cantley, L. C. (1999) *J. Biol. Chem.* **274,** 8347–8350
15. Leevers, S. J., Weinkove, D., MacDougall, L. K., Hafen, E., and Waterfield, M. D. (1996) *EMBO J.* **15,** 6584–6594
16. Shioi, T., Kang, P. M., Douglas, P. S., Hampe, J., Yballe, C. M., Lawitts, J., Cantley, L. C., and Izumo, S. (2000) *EMBO J.* **19,** 2537–2548
17. Damen, J. E., Liu, L., Rosten, P., Humphries, R. K., Jefferson, A. B., Majerus, P. W., and Krystal, G. (1996) *Proc. Natl. Acad. Sci. U. S. A.* **93,** 1689–1693
18. Vanhaesebroeck, B., and Alessi, D. R. (2000) *Biochem. J.* **346,** 561–576
19. Cardone, M. H., Roy, N., Stennicke, H. R., Salvesen, G. S., Franke, T. F., Stanbridge, E., Frisch, S., and Reed, J. C. (1998) *Science* **282,** 1318–1321
20. Brunet, A., Bonni, A., Zigmond, M. J., Lin, M. Z., Juo, P., Hu, L. S., Anderson, M. J., Arden, K. C., Blenis, J., and Greenberg, M. E. (1999) *Cell* **96,** 857–868
21. Hoeflich, K. P., Luo, J., Rubie, E. A., Tsao, M. S., Jin, O., and Woodgett, J. R. (2000) *Nature* **406,** 86–90
22. Dimmeler, S., Fleming, I., Fisslthaler, B., Hermann, C., Busse, R., and Zeiher, A. M. (1999) *Nature* **399,** 601–605
23. Fulton, D., Gratton, J. P., McCabe, T. J., Fontana, J., Fujio, Y., Walsh, K., Franke, T. F., Papapetropoulos, A., and Sessa, W. C. (1999) *Nature* **399,** 597–601
24. Ozes, O. N., Mayo, L. D., Gustin, J. A., Pfeffer, S. R., Pfeffer, L. M., and Donner, D. B. (1999) *Nature* **401,** 82–85
25. Romashkova, J. A., and Makarov, S. S. (1999) *Nature* **401,** 86–90
26. Wang, Q., Somwar, R., Bilan, P. J., Liu, Z., Jin, J., Woodgett, J. R., and Klip, A. (1999) *Mol. Cell. Biol.* **19,** 4008–4018
27. Thorell, A., Hirshman, M. F., Nygren, J., Jorfeldt, L., Wojtaszewski, J. F., Dufresne, S. D., Horton, E. S., Ljungqvist, O., and Goodyear, L. J. (1999) *Am. J. Physiol.* **277,** E733–E741
28. Subramaniam, A., Jones, W. K., Gulick, J., Wert, S., Neumann, J., and Robbins, J. (1991) *J. Biol. Chem.* **266,** 24613–24620
29. Haq, S., Choukroun, G., Kang, Z. B., Ranu, H., Matsui, T., Rosenzweig, A., Molkentin, J. D., Alessandrini, A., Woodgett, J., Hajjar, R., Michael, A., and Force, T. (2000) *J. Cell Biol.* **151,** 117–130
30. Nagata, K., Ye, C., Jain, M., Milstone, D. S., Liao, R., and Mortensen, R. M. (2000) *Circ. Res.* **87,** 903–909
31. Choukroun, G., Hajjar, R., Kyriakis, J. M., Bonventre, J. V., Rosenzweig, A., and Force, T. (1998) *J. Clin. Invest.* **102,** 1311–1320
32. Choukroun, G., Hajjar, R., Fry, S., del Monte, F., Haq, S., Guerrero, J., Picard, M., Rosenzweig, A., and Force, T. (1999) *J. Clin. Invest.* **104,** 391–398
33. Cross, D. A., Alessi, D. R., Cohen, P., Andjelkovich, M., and Hemmings, B. A. (1995) *Nature* **378,** 785–789
34. Kitamura, T., Ogawa, W., Sakaue, H., Hino, Y., Kuroda, S., Takata, M., Matsumoto, M., Maeda, T., Konishi, H., Kikkawa, U., and Kasuga, M. (1998) *Mol. Cell. Biol.* **18,** 3708–3717
35. Shima, H., Pende, M., Chen, Y., Fumagalli, S., Thomas, G., and Kozma, S. C. (1998) *EMBO J.* **17,** 6649–6659
36. Pende, M., Kozma, S. C., Jaquet, M., Oorschot, V., Burcelin, R., Le Marchand-Brustel, Y., Klumperman, J., Thorens, B., and Thomas, G. (2000) *Nature* **408,** 994–997
37. Bodine, S. C., Stitt, T. N., Gonzalez, M., Kline, W. O., Stover, G. L., Bauerlein, R., Zlotchenko, E., Scrimgeour, A., Lawrence, J. C., Glass, D. J., and Yancopoulos, G. D. (2001) *Nat. Cell Biol.* **3,** 1014–1019
38. Pullen, N., Dennis, P. B., Andjelkovic, M., Dufner, A., Kozma, S. C., Hemmings, B. A., and Thomas, G. (1998) *Science* **279,** 707–710
39. Weng, Q. P., Kozlowski, M., Belham, C., Zhang, A., Comb, M. J., and Avruch, J. (1998) *J. Biol. Chem.* **273,** 16621–16629
40. Huang, W. Y., Aramburu, J., Douglas, P. S., and Izumo, S. (2000) *Nat. Med.* **6,** 482–483
41. Rossig, L., Jadidi, A. S., Urbich, C., Badorff, C., Zeiher, A. M., and Dimmeler, S. (2001) *Mol. Cell. Biol.* **21,** 5644–5657
42. Zhou, B. P., Liao, Y., Xia, W., Spohn, B., Lee, M. H., and Hung, M. C. (2001) *Nat. Cell Biol.* **3,** 245–252
43. von Harsdorf, R., Hauck, L., Mehrhof, F., Wegenka, U., Cardoso, M. C., and Dietz, R. (1999) *Circ. Res.* **85,** 128–136
44. Verdu, J., Buratovich, M. A., Wilder, E. L., and Birnbaum, M. J. (1999) *Nat. Cell Biol.* **1,** 500–506
45. Tuttle, R. L., Gill, N. S., Pugh, W., Lee, J. P., Koeberlein, B., Furth, E. E., Polonsky, K. S., Naji, A., and Birnbaum, M. J. (2001) *Nat. Med.* **7,** 1133–1137
46. Bueno, O. F., De Windt, L. J., Tymitz, K. M., Witt, S. A., Kimball, T. R., Klevitsky, R., Hewett, T. E., Jones, S. P., Lefer, D. J., Peng, C. F., Kitsis, R. N., and Molkentin, J. D. (2000) *EMBO J.* **19,** 6341–6350
47. Morisco, C., Zebrowski, D., Condorelli, G., Tsichlis, P., Vatner, S. F., and Sadoshima, J. (2000) *J. Biol. Chem.* **275,** 14466–14475
48. Zhang, H., Stallock, J. P., Ng, J. C., Reinhard, C., and Neufeld, T. P. (2000) *Genes Dev.* **14,** 2712–2724
49. Harada, H., Andersen, J. S., Mann, M., Terada, N., and Korsmeyer, S. J. (2001) *Proc. Natl. Acad. Sci. U. S. A.* **98,** 9666–9670

Phenotypic Spectrum Caused by Transgenic Overexpression of Activated Akt in the Heart

Takashi Matsui, Ling Li, Justina C. Wu, Stuart A. Cook, Tomohisa Nagoshi, Michael H. Picard, Ronglih Liao and Anthony Rosenzweig

J. Biol. Chem. 2002, 277:22896-22901.
